RESEARCH ARTICLE

Non-linear Taylor Instability Analysis for Elliptical and Elliptical Conical Liquid Hollow Jets and its Application for Non-Circular Fuel Injectors

Igor Gaissinski[1,] Vladimir Rovenski[2]

[1]*Faculty Airspace Engineering, TECHNION, Haifa 3200003, Israel,* [2]*Department of Mathematics, Haifa University, Haifa 3498838, Israel*

ABSTRACT

The main goal in the design of injectors is the finest-dispersed and uniform spraying of the liquid. In the case of engines, it gives a dual effect: Increased engine power, fuel economy, and reduction in the concentration of harmful impurities in the exhaust gases. For the processes of thin films spraying, this leads to the saving of expensive materials used for coatings and to obtain a better quality of a surface. A fundamentally this method based on the analysis of non-linear hydrodynamic instability is presented, which allows to determine the optimal shape and dimensions of an injector for a given aircraft/car engine or for deposition of protective shells on surfaces. The present study is a development of our research on the circular shape of a thin liquid film (the main ones are present in [1-4]). By varying the size of the slit for fluid injection and several standard shapes (circular, elliptical with the ratio apogee/perigee, etc.) it is possible to determine at what shape and size of the slit a minimum film breaking time is achieved. Exact hydrodynamic solutions, obtained by this method, may be tabulated to determine input parameters and modes of more optimal injectors, and, as the result, to increase the efficiency of injectors design. The method is based on our completely new physical model, explaining, predicting, and estimating sufficiently non-linear instability of interacting flows. In particular, the instability analysis results are obtained for the elliptically cylindrical and elliptically conical shapes of atomizers. It is shown that atomizers with elliptical nozzle shapes are more effective than atomizers with circular nozzle shapes; their times of the film destruction differ 18 times. The main goal in the construction and design of injectors is the finest-dispersed and uniform spraying of the liquid. In the case of engines, it has a dual effect: increasing of engine power, fuel economy, and decreasing the concentration of harmful impurities in exhaust gases. Software based on the developed theory, will eliminate some work of designers and provide better design of atomizers.

Key words: Hydrodynamic instability, Taylor instability, hollow jet, liquid film, injector, aircraft engine, motion equation, Lagrange coordinates, conical elliptical film

INTRODUCTION

A method based on a hydrodynamic instability non-linear analysis of a thin liquid film with be disclosed. Exact hydrodynamic solutions, obtained by this method, can be tabulated to determine input parameters and modes of more optimal injectors, and, as the result, to increase the efficiency of injectors design. The present study can be considered as a development of our research for circular shape of a thin liquid film.[1-4]

HYDRODYNAMIC INSTABILITY MODEL

A fundamentally this method based on the analysis of non-linear hydrodynamic instability is presented, which allows the designer to determine the optimal shape (circular, elliptical, etc.) and dimensions of an injector for

Address for correspondence:
Igor Gaissinski
E-mail: ricka1993@012.net.il

a given aircraft/car engine or for deposition of protective shells on surfaces. The program that implements this method has an interface allowing the designer in a few minutes to enter the principal sizes (nozzle diameter and width of the slit for liquid injection) of the injector and the initial parameters (longitudinal and swirling velocities) to find the characteristic time for the beginning of the film destroy. Varying the size of the slit for fluid injection and several standard shapes (circular, elliptical with the ratio apogee/perigee, etc.) makes it possible to determine at what shape and size of the slit a minimum film breaking time is achieved. Exact hydrodynamic solutions, obtained by this method, may be tabulated to determine input parameters and modes of more optimal injectors, and as the result to increase the efficiency of injectors design.

The surface between the shell and the outer medium consists of two or, in the case of liquid film, of three regions [Figure 1]: The area of occurrence (I) and the development of (II) unstable modes, III – the region of the liquid film destruction and the beginning of atomization process.

The present method is based on the motion equation[5] of a shell or thin liquid film [Figures 2 and 3]:

$$\rho \partial_{tt}^2 \mathbf{r} = \Delta p \cdot \left(\mathbf{e}_z \times \partial_\psi \mathbf{r} \right), \tag{1}$$

where the density ρ and the pressure difference Δp between external and internal media are assumed to be constant, ψ is a Lagrange coordinate, that is, $d\psi = \pi R_0^2 d\phi$ per unit of the length in $\mathbf{e}_z$ direction, with $\phi \in [0,1]$ – dimensionless azimuth angle and, R_0 – the initial generalized radius of the shell. Substitution $\mathbf{r} = [Z, 0]$, $Z = X + iY \in \mathbb{C}$ transforms (1) to the PDE for $Z(\phi, t)$,
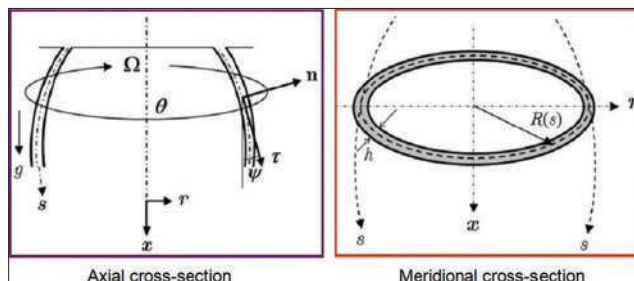
$$\partial_{tt}^2 Z = i \left[\Delta p / (\pi \rho R_0^2) \right] \partial_\phi Z, \tag{2}$$
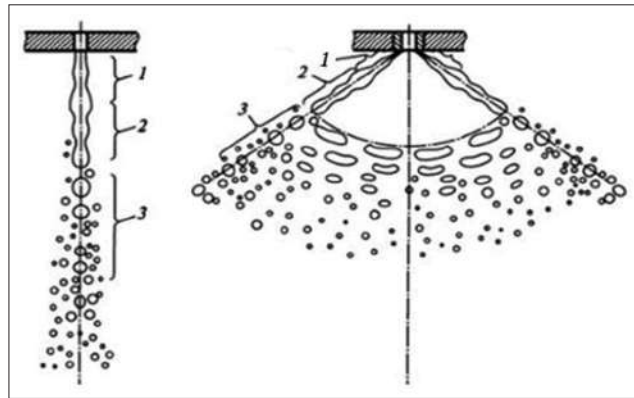
Figure 1: The structure of the shell: Zone 1 is the beginning of the phenomenon of surface waves, zone 2 is the development of instability, and zone 3 (exists only in the case of liquid film) is destruction of the film (atomization)
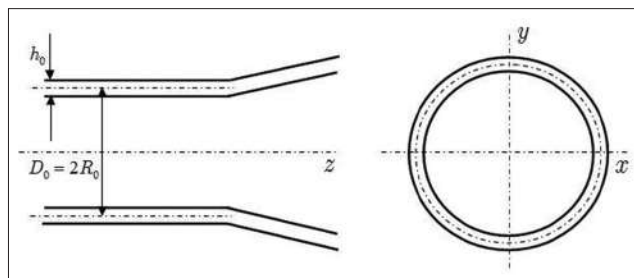
Figure 2: The schema of injector with circular cross-section (for the case of liquid film)

Figure 3: The schematic view of the liquid film with coordinates

which is equivalent to the system of linear PDEs for real and imaginary parts of $Z(\varphi,t)$,

$$\partial^2_{tt} X = -\left[\Delta p / (\pi \rho R_0^2)\right]\partial_\phi Y, \quad \partial^2_{tt} Y = \left[\Delta p / (\pi \rho R_0^2)\right]\partial_\phi X \tag{3}$$

In general, we assume $Z(\phi,0)$ to be given and

$$\partial_t Z(\phi,0) = \Omega Z(\phi,0) \tag{4}$$

Breakthrough of the invention is our novel assumption that the shell has an elliptical cylinder shape, with the ellipse (cross-section) equation of unit generalized radius

$$z(\phi) = (\cos\theta \cos\phi + i \sin\theta \sin\phi), \quad \theta = \arctan(b/a).$$

Here, α, b ($\alpha>b$) are semi-axes of elliptical cross-section of the shell. Similarly to solutions for a shell of circular shape, $Z_k(\phi,t) = R(t)\left[\exp(i\phi) - \lambda(t)k^{-1}\exp(ik\phi)\right]$ with the wave number $k \in \mathbb{Z}/\{0\}$ and the initial instability increment $\lambda(0)=\lambda_0$ such that $|\lambda_0|$ is sufficiently smaller than unit, see (1, 2), we are looking for particular solutions of (3) in the form

$$X_k(\phi,t) = R_+(t)\left(\cos\phi - \lambda_+(t)k^{-1}\cos k\phi\right),$$
$$Y_k(\phi,t) = R_-(t)\left(\sin\phi - \lambda_-(t)k^{-1}\sin k\phi\right) \tag{5}$$

with the initial conditions, see (4),

$$X_k(\phi,0) = a\cdot(\cos\phi - \lambda_0 k^{-1}\cos k\phi), \partial_t X_k(\phi,0) = \Omega X_k(\phi,0),$$
$$Y_k(\phi,0) = b\cdot(\sin\phi - \lambda_0 k^{-1}\sin k\phi), \partial_t Y_k(\phi,0) = \Omega Y_k(\phi,0). \tag{6}$$

This is equivalent to solution $Z_k(\phi,t)=X_k(\phi,t)+iY_k(\phi,t)$ of (2),

$$Z_k(\phi,t) = R(t)\Psi_k(\phi,t), \Psi_k(\phi,t) = [z(\phi) - \lambda(t)k^{-1}z(k\phi)]. \tag{7}$$

Here, $R(t)$ and $\psi_k(\phi,t)$ ($k \in \mathbb{Z}/\{0\}$) are the radial and angular parts of the solution. An analogy of (7) with the solution for a circular shape is shown in Figure 4.

In the case of liquid film, the shell may rotate with initial angular velocity $\Omega=V_{\phi0}/R_0$ [Figure 3], where $V_{\phi0}$ is the swirl velocity, $R_0=(a^2+b^2)^{1/2}$, and the radial velocity is zero. In our case, by comparison with a circular cylindrical shell, the initial angular velocity Ω has sufficient limitation [Appendix 1]:

$$\Omega < R_0^{-1}\sqrt{\sigma/\rho}.$$

Substituting (5) into (3), grouping the terms $\{\cos\phi, \cos k\phi\}$ and $\{\sin\phi, \sin k\phi\}$, and passing to dimensionless variables, we obtain the system of four ODE's for functions $R_+, \lambda_+, R_-, \lambda_-$ of τ:

$$\frac{d^2\tilde{R}_\pm}{d\tau^2} + A\tilde{R}_\mp = 0 \tag{8a}$$

$$\frac{d^2\lambda_\pm}{d\tau^2} + \frac{2}{R_\pm}\frac{d\tilde{R}_\pm}{d\tau}\frac{d\lambda_\pm}{d\tau} + A\frac{\tilde{R}_\mp}{\tilde{R}_\pm}\left(k\lambda_\mp - \lambda_\pm\right) = 0 \tag{8b}$$
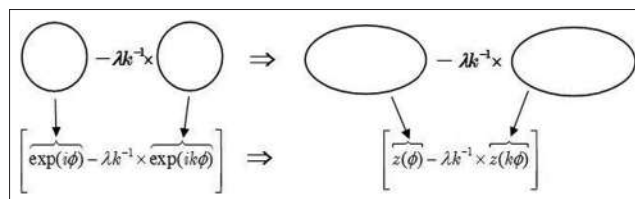
Figure 4: Converting the solution type from circular to elliptical shape of the film

with initial conditions

$$\tilde{R}_+(0) = \cos\theta, \quad \tilde{R}_-(0) = \sin\theta, \quad dR_+/d\tau\big|_{\tau=0} = V_\Omega \cos\theta, \quad d\tilde{R}_-/d\tau_{\tau=0} = V_\Omega \sin\theta, \tag{9a}$$

$$\lambda_\pm(0) = \lambda_0, \quad d\lambda_\pm/d\tau\big|_{\tau=0} = 0. \tag{9b}$$

Here, $R_\pm(t) = R_0 \tilde{R}_\pm(\tau)$, $\tau = t/t_0$, $V_\Omega = V_{\varphi 0}/V_{z0}$, $A = \pi^{-1}\Delta p/(\rho V_{z0}^2) = (2\pi)^{-1}(\Delta p_{\text{stat}}/\Delta p_{\text{dyn}})$ is the static,

$\Delta p_{\text{stat}} \equiv \Delta p$, and dynamic, $\Delta p_{\text{dyn}} = \frac{1}{2}\rho V_{z0}^2$, pressure ratio, where, in the case of liquid film, $t_0 = R_0/V_{z0}$ and

V_{z0} are the characteristic time of the motion and the initial axial velocity of the liquid film.

One may write $A = \pi^{-1}(h_0/R_0)\, \text{Lf}$, where $\text{Lf} = \text{Eu}/\text{We}$ is the *Lefebvre number* named after Lefebvre by the authors.[2-4] Here, $\text{Eu} = \Delta p R_0/2\sigma_*$ is the Euler number, $\text{We} = \rho h_0 V_{z0}^2/2\sigma_*$ is the Weber number, σ_* – the surface tension coefficient, h_0 – the shell thickness. The Lefebvre number means the ratio of static and dynamic pressures.

For the case of solid shell, one should use another value

$$A_{\text{solid}} = \frac{1}{\pi(b/a)}\frac{\Delta p_0}{(a/t_0)^2\rho} \text{ instead of } A = \pi^{-1}\Delta p/(\rho V_{z0}^2) = (2\pi)^{-1}(\Delta p_{\text{stat}}/\Delta p_{\text{dyn}}),$$

where t_0 is the characteristic time that may be considered as the time requested to put the rocket into near-earth orbit that is equal to 600–700 s. Due to $a \approx 4.35\,\text{m}$, $\Delta p_0 \approx 0 \div 10^5\,\text{Pa}$ (the maximal pressures 10^5Pa corresponds to the temperature at the earth surface, T_{EARTH}, to be assumed 300K), and $\rho = \rho_{\text{Shell}} \approx 2640\,\text{kg/m}^3$, the value $A_{\text{solid}} \approx 2.324 \times 10^5 \cdot (a/b)$.

By (8a) and (9a), the calculation formulae for the radial functions $R_\pm(\tau)$ are

$$\tilde{R}_\pm = \begin{cases} \frac{1}{2}\Big\{\Big[\big(\cos\sqrt{A}\tau \pm \cosh\sqrt{A}\tau\big) + V_\Omega A^{-1/2}\big(\sin\sqrt{A}\tau \mp \sinh\sqrt{A}\tau\big)\Big]\cos\theta \\ \quad + \Big[\big(\cos\sqrt{A}\tau \mp \cosh\sqrt{A}\tau\big) + V_\Omega A^{-1/2}\big(\sin\sqrt{A}\tau \pm \sinh\sqrt{A}\tau\big)\Big]\sin\theta\Big\}, & \Delta p > 0 \\[2mm] \begin{pmatrix}\cos\theta \\ \sin\theta\end{pmatrix}\cdot(V_\Omega\tau + 1), & \Delta p = 0 \\[2mm] \frac{1}{2}\Big\{\Big[\big(\cosh\sqrt{|A|}\tau \pm \cos\sqrt{|A|}\tau\big) + V_\Omega|A|^{-1/2}\big(\sinh\sqrt{|A|}\tau \mp \sin\sqrt{|A|}\tau\big)\Big]\cos\theta \\ \quad + \Big[\big(\cosh\sqrt{|A|}\tau \mp \cos\sqrt{|A|}\tau\big) + V_\Omega|A|^{-1/2}\big(\sinh\sqrt{|A|}\tau \pm \sin\sqrt{|A|}\tau\big)\Big]\sin\theta\Big\} & \Delta p < 0 \end{cases} \tag{10}$$

Hence, their derivatives are given by

$$\frac{d\tilde{R}_\pm}{d\tau} = \begin{cases} -\frac{\sqrt{A}}{2}\Big\{\Big[\big(\sin\sqrt{A}\tau \mp \sinh\sqrt{A}\tau\big) + V_\Omega A^{-1/2}\big(\cos\sqrt{A}\tau \mp \cosh\sqrt{A}\tau\big)\Big]\cos\theta \\ \quad + \Big[\big(\sin\sqrt{A}\tau \pm \sinh\sqrt{A}\tau\big) - V_\Omega A^{-1/2}\big(\cos\sqrt{A}\tau \pm \cosh\sqrt{A}\tau\big)\Big]\sin\theta\Big\}, & \Delta p > 0 \\[2mm] \begin{pmatrix}\cos\theta \\ \sin\theta\end{pmatrix}\times V_\Omega, & \Delta p = 0 \\[2mm] \frac{\sqrt{|A|}}{2}\Big\{\Big[\big(\sinh\sqrt{|A|}\tau \mp \sin\sqrt{|A|}\tau\big) + V_\Omega|A|^{-1/2}\big(\cosh\sqrt{|A|}\tau \mp \cos\sqrt{|A|}\tau\big)\Big]\cos\theta \\ \quad + \Big[\big(\sinh\sqrt{|A|}\tau \pm \sin\sqrt{|A|}\tau\big) + V_\Omega|A|^{-1/2}\big(\cosh\sqrt{|A|}\tau \pm \cos\sqrt{|A|}\tau\big)\Big]\sin\theta\Big\}. & \Delta p < 0 \end{cases} \tag{11}$$

Then, the solution $\lambda_+(\tau)$, $\lambda_-(\tau)$ (the increments) of the linear system (8b) and (9b) can be found numerically. Finally, we get the solution of the form (5) to the system (3):

Given t, the graph of $Z_k(\phi,t)$ becomes a cycloidal curve (hypocycloid for $k>0$ with $k-1$ singular points, and epicycloid for $k<0$ with $|k-1|$ singular points, when $|\lambda(t)|=1$ at $t=t_*$), depending on the sign of the wave number k [Figures 5 and 6]. Indeed, for round cylindrical shell, when $Z_k(\phi,t)=R(t)[\exp(i\phi)-k^{-1}\exp(ik\phi)]$, we have $\partial_\phi Z_k = iR(t)\exp(i\phi)\left[1-\exp\{i(k-1)\phi\}\right]$, thus the inequality $1-\exp\{i(k-1)\phi\}\geq 0$ has zeros (the critical points) $\phi = 2\pi / |k-1|$, and their number is $n = |k-1|$.

For elliptic cylindrical shell, we have $\partial_\phi Z_k = 2R(t)\sin\left\{\frac{1}{2}(k-1)\phi\right\}\cos\left\{\theta-\frac{1}{2}(k+1)\phi\right\}\geq 0$, and this inequaliy shows, similarly with the previous case, the same number $n = |k-1|$ of zeros (the critical points).

RESULTS AND DISCUSSION

The dependencies of increments $\lambda_\pm=\lambda_\pm(\tau)$ on the dimensionless time τ are presented in Figures 7-18, where the solid line corresponds to λ_+, and the dash one – to λ_-. The times of the liquid film destruction
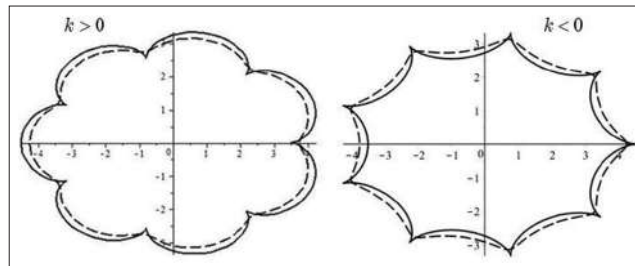

Figure 5: The perturbed form Z_k for $k=\pm8$ (with initial generalized radius to be unit) for the shell of elliptical cross-section (epi- and hypo- cycloids): for $\lambda_\pm=0.5$ (dash line) and for $\lambda_\pm=1$ (solid line)
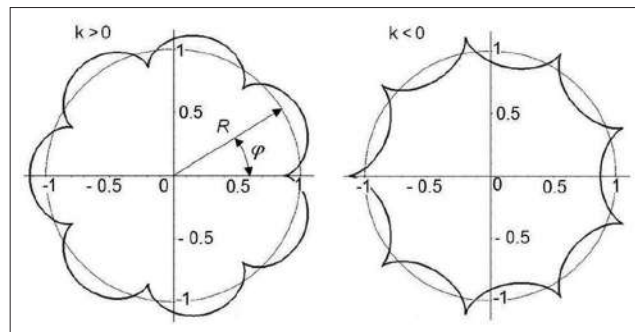

Figure 6: The perturbed form Z_k for $k=\pm8$ (with unit radius) for the shell of circular cross-section for $\lambda=1$ and $k=\pm8$, $\phi=2\pi\phi$
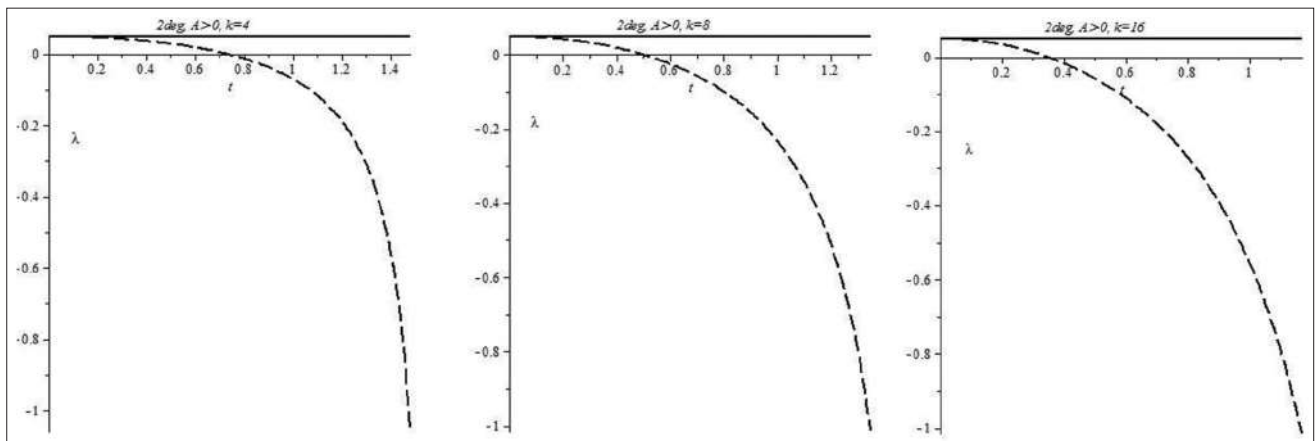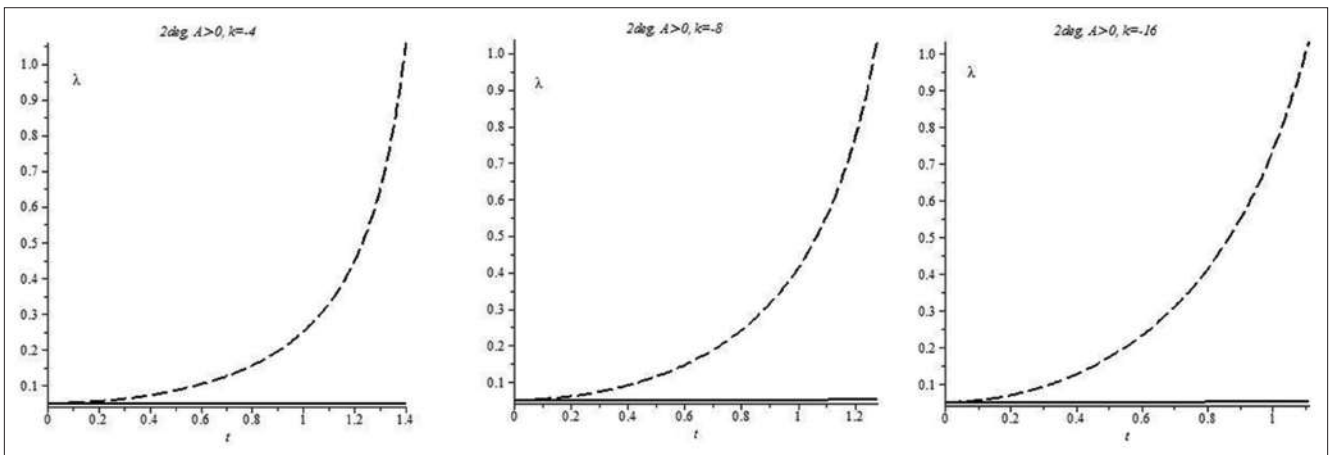

Figure 7: The amplitudes for the film with elliptical cross-section shape are shown for three positive wave numbers, $k=4$, 8, 16, for $\Delta\rho>0$ ($A=0.04$), $V_\Omega=0.001$ and $\theta=2^0$
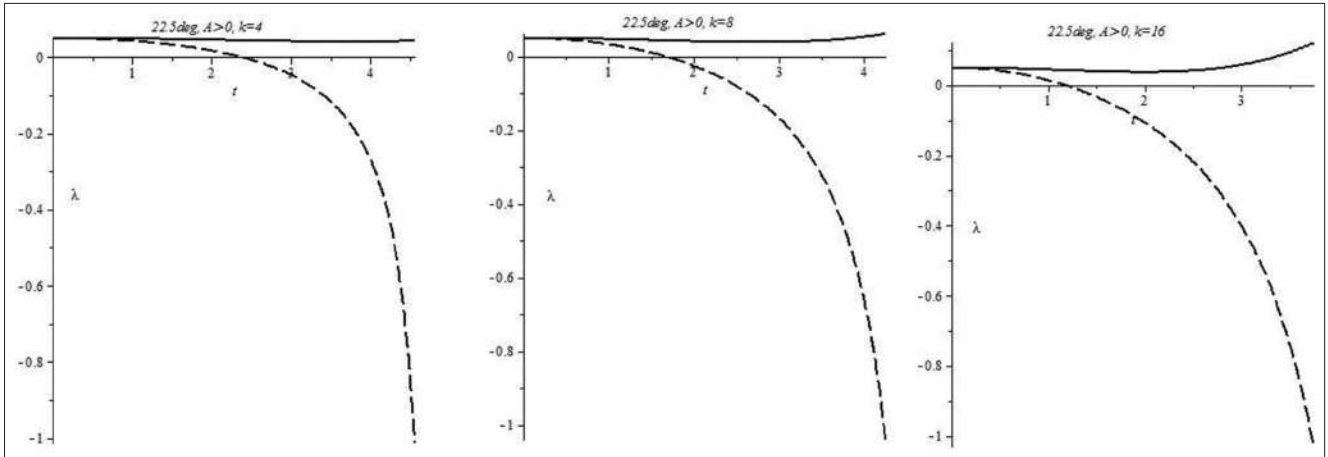
Figure 8: The amplitudes for the film with elliptical cross-section shape are shown for three positive wave numbers, k=4, 8, 16, for $\Delta\rho$>0 (A=0.04), V_Ω=0.01 and θ=22.5^0
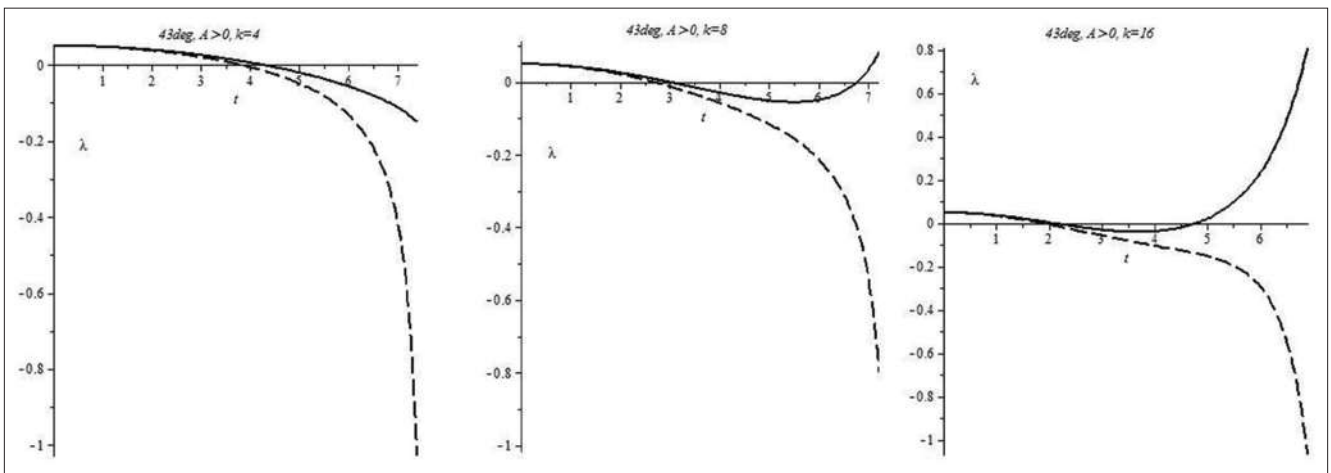
Figure 9: The amplitudes for the film with elliptical cross-section shape are shown for three positive wave numbers, k=4, 8, 16, for $\Delta\rho$>0 (A=0.04), V_Ω=0.01 and θ=43.0^0
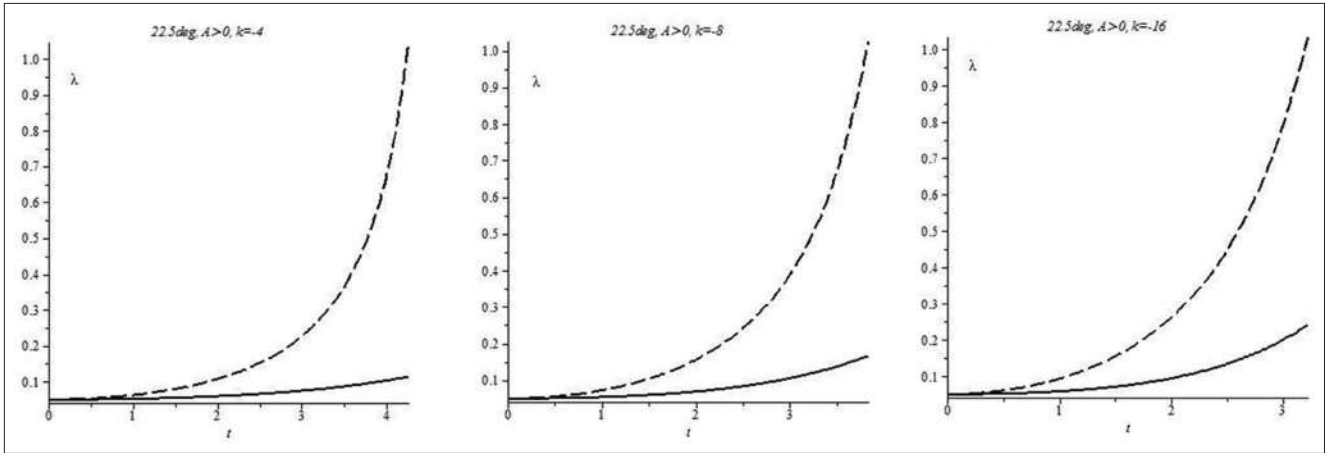

Figure 10: The amplitudes for the film with elliptical cross-section shape are shown for three negative wave numbers, k=−4, −8, −16, for $\Delta\rho$>0 (A=0.04), V_Ω=0.01 and θ=2^0

corresponding to these graphs are shown in Figure 19.

We presented results only for the wave numbers k=4, 8, and 16, because for k>16 one obtains the similar result, while long-wave modes, with k<4, do not appear initially.

The main results are tabulated in Table 1. It shows depending the characteristic time τ_* when the graphs $\lambda_\pm$ intersect the value $\left|\lambda_\pm\right|=1$ on the calculation variant [Figures 7-18].

Figure 11: The amplitudes for the film with elliptical cross-section shape are shown for three negative wave numbers, $k=-4, -8, -16$, for $\Delta\rho>0$ ($A=0.04$), $V_\Omega=0.01$ and $\theta=22.5^0$
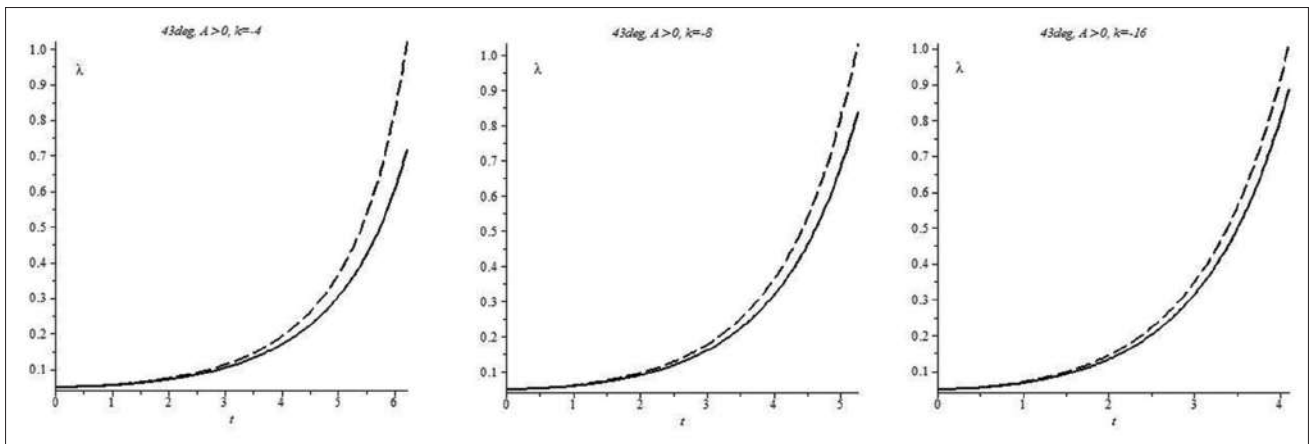
Figure 12: The amplitudes for the film with elliptical cross-section shape are shown for three negative wave numbers, $k=-4, -8, -16$, for $\Delta\rho>0$ ($A=0.04$), $V_\Omega=0.01$ and $\theta=43.0^0$
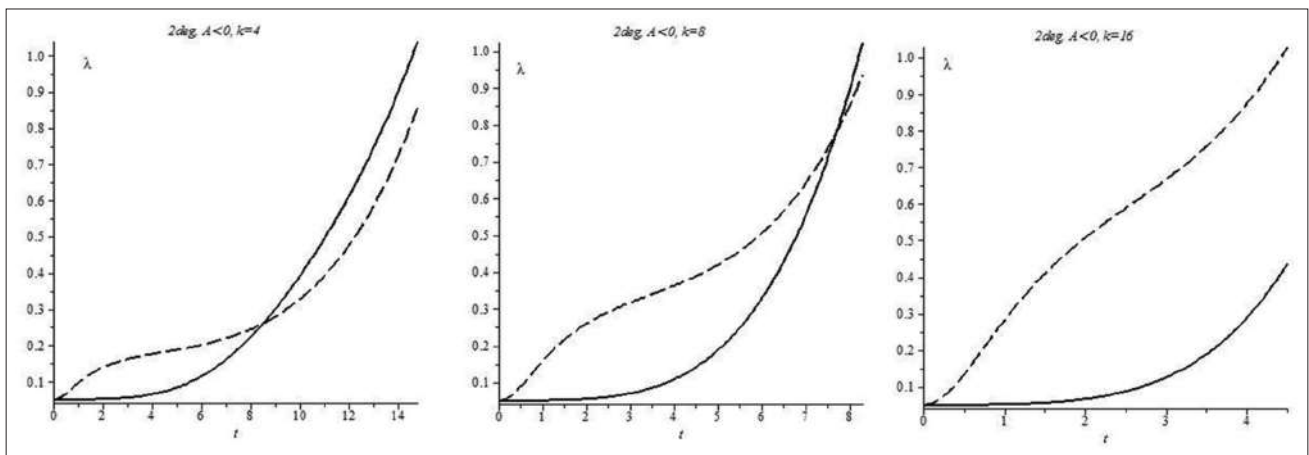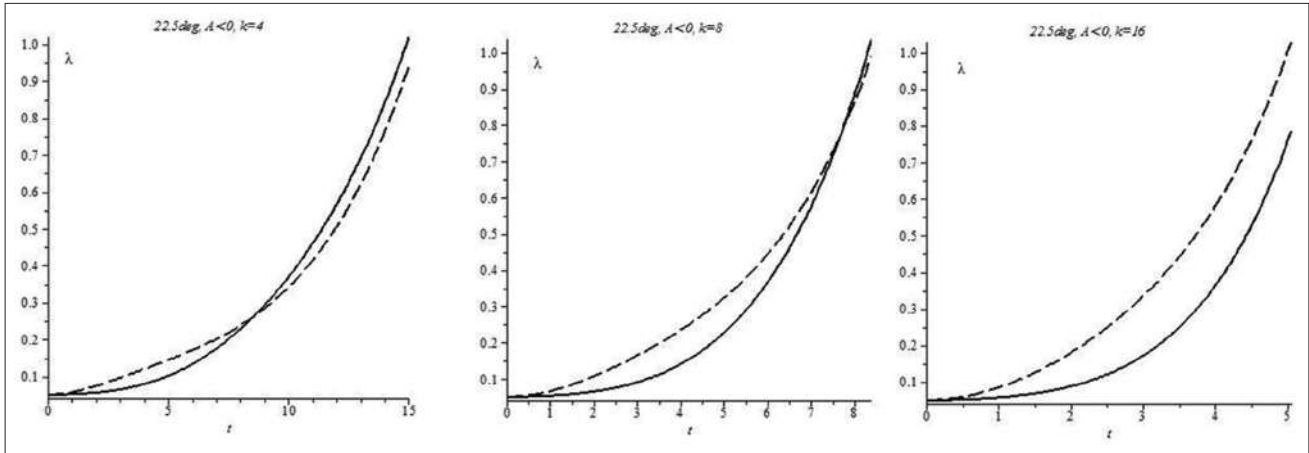

Figure 13: The amplitudes for the film with elliptical cross-section shape are shown for three positive wave numbers, $k=4$, 8, 16, for $\Delta p < 0$ ($A = -0.04$), $V_\Omega=0.01$ and $\theta=2^0$

The characteristic time τ^*, placed in the last row of Table 1 has three values corresponding to each value of the wave number $k=4$, 8, and 16 placed at the above row of the same table.
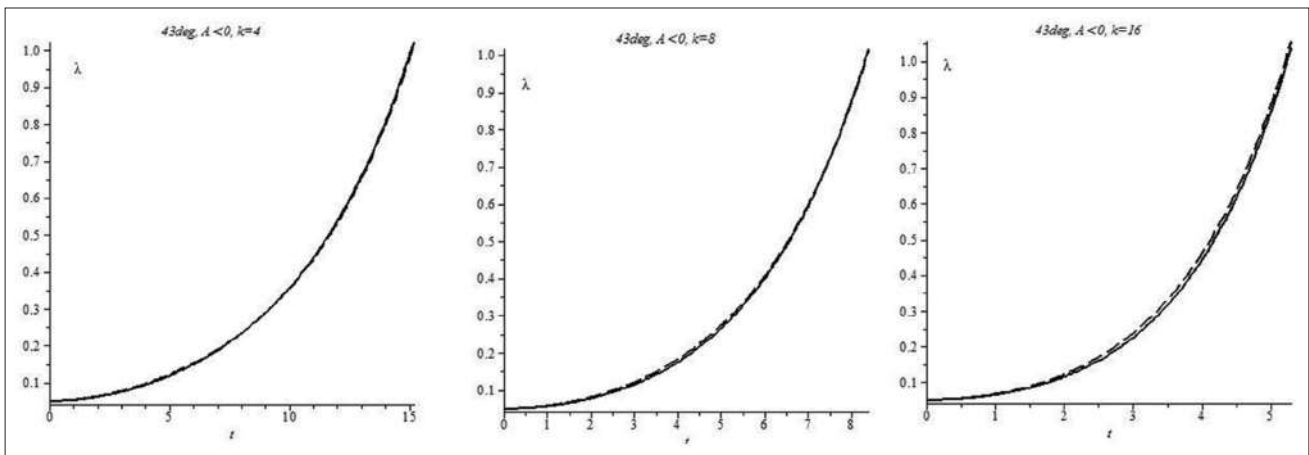
The fastest destruction of a liquid film occurs in cases 1–6, that is, for positive pressure drops, $\Delta\rho>0$, moreover, for low values θ [Figures 1-4], that is, for more elongated ellipse, when α>>b.
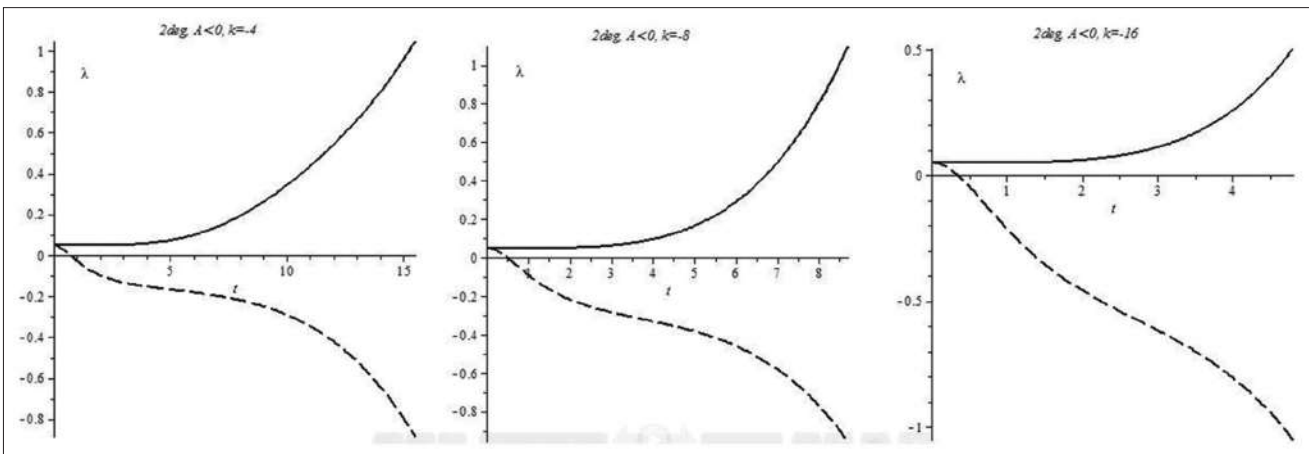
The useful histogram is shown in Figure 19.

For comparison, there are present results for the liquid film of cylindrical shape [Figure 20]. For negative pressure drop and negative wave numbers $k < 0$ the film even, it does not collapse.

Figure 14: The amplitudes for the film with elliptical cross-section shape are shown for three positive wave numbers, k=4, 8, 16, for $\Delta p < 0$ $(A = -0.04)$, V_Ω=0.01 and θ=22.5^0

Figure 15: The amplitudes for the film with elliptical cross-section shape are shown for three positive wave numbers, k=4, 8, 16, for $\Delta p < 0$ $(A = -0.04)$, V_Ω=0.01 and θ=43.0^0
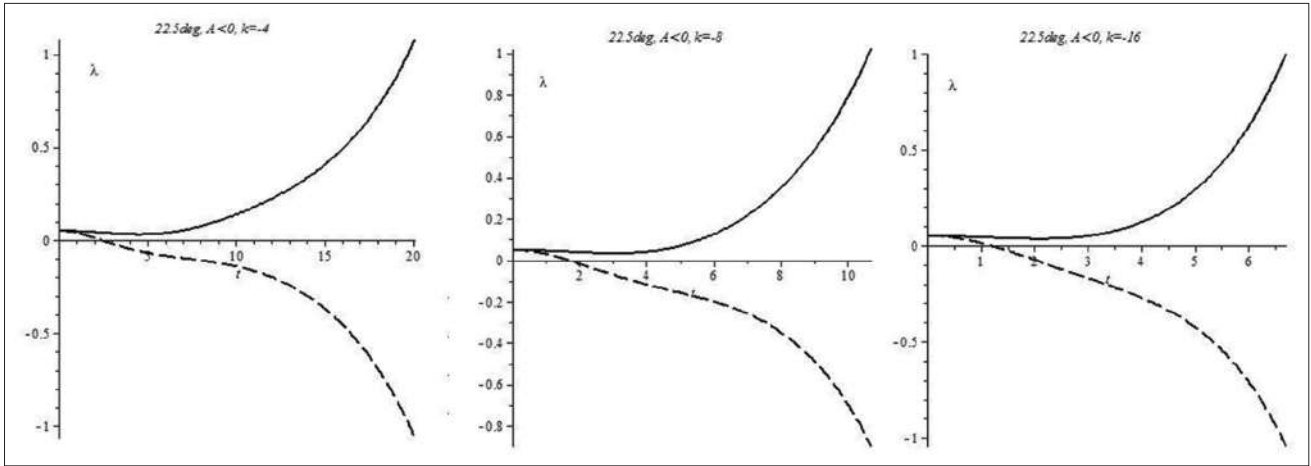

Figure 16: The amplitudes for the film with elliptical cross-section shape are shown for three positive wave numbers, k=−4, −8, −16, for $\Delta p < 0$ $(A = -0.04)$, V_Ω=0.01 and θ=2^0

In the case of the conical form (instead of cylindrical) of the surface when $a_L = a + L\tan\alpha$, where a is a half of the conical angle, and L is the distance downstream of the injector's nozzle, we use new coefficients, A_L and B_L, for every cross-sections placed at the distance L downstream the nozzle and obtain the new results $\lambda_\pm(\tau,L)$ depending on L as follows (Appendix 2),

$$A_L = \pi^{-1}\Delta p / \left(\rho V_{z0}^2\right) = \pi^{-1}\left(h_0 / R_0\right)\left[1 + (L / a)\tan\alpha\right]^{-1} \mathrm{Lf}, \quad B_L = V_\Omega / \sqrt{|A_L|}$$
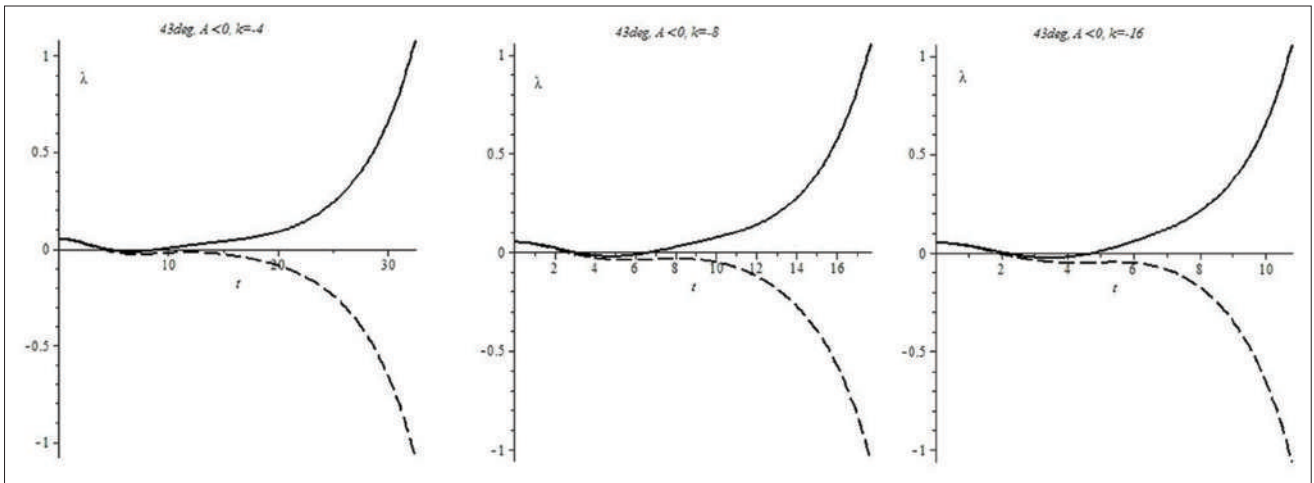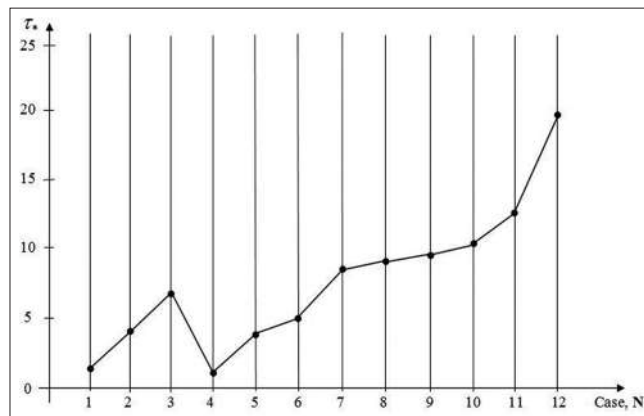
Figure 17: The amplitudes for the film with elliptical cross-section shape are shown for three positive wave numbers, k=−4, −8, −16, for $\Delta p < 0$ $(A = -0.04)$, V_Ω=0.01 and θ=22.5^0

Figure 18: The amplitudes for the film with elliptical cross-section shape are shown for three positive wave numbers, k=−4, −8, −16, for $\Delta p < 0$ $(A = -0.04)$, V_Ω=0.01 and θ=43.0^0

Figure 19: The averaged (over the wave number k) times of the film destruction corresponded to the example presented in Figure 6; here $\tau_* = t_* / t_0$, t_* is the liquid film destruction time.

APPLICATIONS AND NOVELTY

The main objects are injectors of aircrafts and rockets engines, auto motors (piston engines), deposition of protective shells on surfaces, spraying.

The product is based on our completely new physical model, explaining, predicting and estimating instabilities of interacting flows. Until now, there was no good theory to describe these instability phenomena (determined by differences of pressure, temperature, velocity, density etc.), that's why

Table 1: The characteristic time τ_* when the graphs $\lambda_\pm$ intersect the value $\left|\lambda_\pm\right| = 1$

Case	1	2	3	4	5	6	7	8	9	10	11	12
Figures	7	8	9	10	11	12	13	14	15	16	17	18
A	0.04	0.04	0.04	0.04	0.04	0.04	−0.04	−0.04	−0.04	−0.04	−0.04	−0.04
V_Ω	0.01	0.01	0.01	0.01	0.01	0.01	0.01	0.01	0.01	0.01	0.01	0.01
θ	2^0	22.5^0	43.0^0	2^0	22.5^0	43.0^0	2^0	22.5^0	43.0^0	2^0	22.5^0	43.0^0
K	4,8,16	4,8,16	4,8,16	−4,−8,16	−4,−8,−16	−4,−8,−16	4,8,16	4,8,16	4,8,16	−4,−8,−16	−4,−8,−16	−4,−8,−16
τ_*	1.4;1.3;1.1	5;4;3.5	7;7;6.5	1.3;1.2;1.1	4;3.8;3	6;5;4	14;8;4	15;8;5	15;8;5	15;9;5	20;11;9	32;17;1
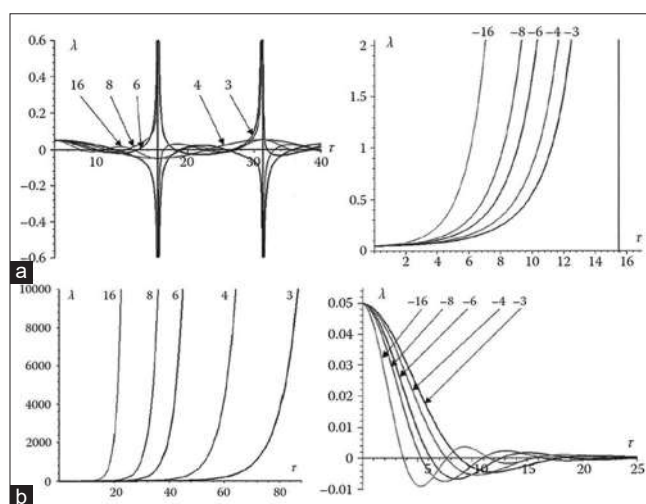
Figure 20: (a-b) The amplitudes for the circular cross-section shape are shown for $\Delta\rho>0$; the left figure is for positive wave numbers k=4, 8, and 16, while the right figure is for negative wave numbers k=−4, −8, and −16

their modeling was not available for designers of injectors in critical industries such as automotive, spacecraft and aircraft, and the process industries, where injectors are used extensively in food, medical, and chemical industries. The lack of such models caused designers to put extra means ("over design") in constructions to ensure their reliability. Software, based on the developed theory, will close this gap, will eliminate some work done by designers and ensure better design. As a result, significant saving can be achieved in production and/or operation.

The main goal in the design and construction of injectors is the finest-dispersed and uniform spraying of the liquid. In the case of engines, it has a double effect: to increase of engine power, fuel economy, and to decrease the concentration of harmful impurities in the exhaust gases. For thin-film spraying processes, this results in savings in expensive materials used for coatings, as well as in obtaining a better quality of a surface.

INSTEAD OF CONCLUSION

Even in early childhood, at the age of five, I noticed that the water flow coming out of the irrigation hose with a cylindrical nozzle flows smoothly, and vice versa, when using a hose with a highly compressed elliptical nozzle, a jet is sprayed, almost instantly apparently, these childhood memories prompted me to this study. / Igor Gaissinski /.

REFERENCES

1. Gaissinski I, Levy Y, Rovenski V, Sherbaum V. Rotational liquid film interacted with ambient gaseous media. Vol. 72. In: Geometry and its Applications, Springer Proceedings, Mathematics and Statistics; 2014. p. 199-224.
2. Gaissinski I, Levy Y, Sherbaum V, Kutikov D, Rovenski V. Theoretical and Experimental Study of Airblast Atomizer. The 57th Annual Conference on Aerospace Sciences, Proceedings, Israel. Vol. 2; 2017. p. 740-767.

3. Gaissinski I, Levy Y, Kutikov D, Sherbaum V, Rovenski V. Operation study of miniature airblast atomizer under very low liquid pressures. Int J Turbo Jet Eng, 2017; Vol. 36, p. 1-23.
4. Gaissinski I, Rovenski V. Modeling in Fluid Mechanics: Instabilities and Turbulence. Boca Raton, London: CRC Press; 2018. 507p.
5. Gaissinski IM, Kalinin AV, Stepanov AE. Impact of Magnetic field on braking of the α-particles. Sov J Appl Mech Tech Phys 1979; N 6: p. 40-46.

APPENDICES

Appendix 1
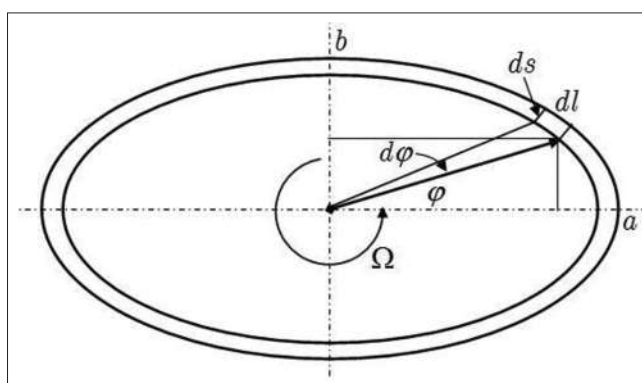
Figure A1: The condition of elliptical film rotation without torn

For the ellipse $a^{-2}x^2 + b^{-2}y^2 = 1$, we have $x = a\cos\varphi$, $y = b\sin\varphi$ [Figure A1]
$r(\varphi) = (b^{-2}\sin^2\varphi + a^{-2}\cos^2\varphi)^{-1/2}$.

The surface tension force is $F_\sigma = \sigma ds = \sigma h_0 d\varphi dz$, where $ds = h_0 dz$ is the square of the film cross-section with the element length dz along z-axis orthogonal to the plane XOY, h_0 is the film thickness.

The centrifugal force F_Ω for the volume element $dV = h_0 dl dz$ of the liquid film is equal

$$F_\Omega = \rho h_0 \Omega^2 r(\varphi) dl dz = \rho h_0 \Omega^2 (b^{-2}\sin^2\varphi + a^{-2}\cos^2\varphi)^{-1} d\varphi dz$$

due to $dl = r(\varphi)d\varphi$. When $F_\Omega \geq F_\sigma$, the film torn, that is, the condition for the film to be conserved is

$$\Omega^2 < (\sigma/\rho)\left(b^{-2}\sin^2\varphi + a^{-2}\cos^2\varphi\right), \text{ for } \varphi \in [0,\ 2\pi].$$

Since $a^{-2} \leq b^{-2}\sin^2\varphi + a^{-2}\cos^2\varphi \leq b^{-2}$, the required condition is $\Omega < a^{-1}\sqrt{\sigma/\rho}$ (for $\varphi_{min} = 0,\ \pi$) consistent to minimum of $b^{-2}\sin^2\varphi + a^{-2}\cos^2\varphi$. For $a = b = R_0$ the above inequality reads as $\Omega < R_0^{-1}\sqrt{\sigma/\rho}$.

Appendix 2
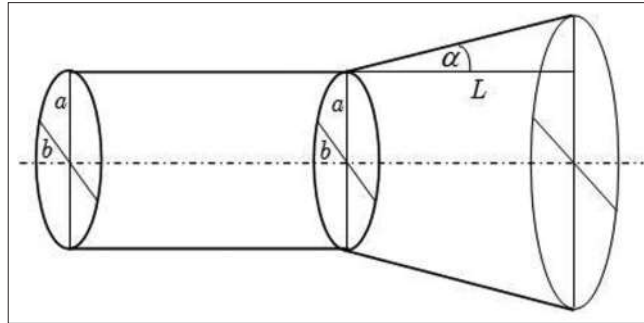
Figure A2: Conical cylinder

For semi-axes of elliptical cross-sections, see Figure A2, we have $a_L = a + L \tan \alpha$, and $b_L = a + L \tan \varphi$. Hence, $R_0 = \sqrt{ab} = a\sqrt{\tan \phi}$ and $R_L = \sqrt{a_L b_L} = (a + L \tan \alpha)\sqrt{\tan \phi} = (a + L \tan \alpha)\sqrt{b/a}$. As a result

$$R_L / R_0 = (a + L \tan \alpha)\sqrt{b/a} / \left(a\sqrt{b/a}\right) = \left[1 + (L/a)\tan \alpha\right] \quad \Rightarrow \quad R(L) = R_0\left[1 + (L/a)\tan \alpha\right], \quad \text{and}$$

$$A_L = \pi^{-1}\left(h_0 / R_L\right)\mathrm{Lf} = \pi^{-1}h_0\left[(a + L \tan \alpha)\sqrt{b/a}\right]^{-1}\mathrm{Lf} = \pi^{-1}\left(h_0 / R_0\right)\left[1 + (L/a)\tan \alpha\right]^{-1}\mathrm{Lf}.$$